Contrib Mineral Petrol (1999) 137: 1–14

Andreas Audétat · Detlef Günther

Mobility and H_2O loss from fluid inclusions in natural quartz crystals

Received: 17 November 1998 / Accepted: 16 April 1999

Abstract Petrographic observations on quartz crystals from the Mole Granite (Australia) and other localities shed new light on the mechanisms of post-entrapment modification of fluid inclusions. These modifications include migration away from pseudosecondary trails, changes in fluid salinity and density, shape distortion and the formation of "sweat-haloes" around strongly deformed inclusions. Increases in fluid salinity, which usually are associated with inclusion migration, indicate water-losses of up to 50%. However, LA-ICP-MS-analysis of unmobilized and mobilized inclusions of the same trail reveals basically unchanged ratios of major – and trace element cations, with the exception of Li, which seems to be incorporated into the crystal lattice during migration. Despite the fact that all these modifications are closely related to deformation processes, they occur not only in mechanically deformed quartz, but also in free-standing crystals. In the latter samples, stress has been generated internally as a result of brazil-twinned growth and compositional zonation. These observations and their interpretation leads to a list of practical criteria that should help in differentiating between reliable and suspect fluid inclusions in other samples.

A. Audétat (✉)
Institute for Isotope Geology, ETH Zentrum/NO,
CH-8092 Zürich, Switzerland
e-mail: audetat@erdw.ethz.ch, Tel.: +41-1-6326082,
Fax: +41-1-6321179

D. Günther
Laboratory of Inorganic Chemistry, ETHZ,
Universitätsstrasse 6, CH-8092 Zürich, Switzerland
e-mail: guenther@inorg.chem.ethz.ch, Tel.: +41-6324687,
Fax: +41-1-6321090

Editorial responsibility: V. Trommsdorff

Introduction

Fundamental to most fluid inclusion studies is the assumption that fluid inclusions behave as compositionally and volumetrically closed systems after the time of their formation. Even if this assumption is reasonable in many cases (Roedder 1984), it is not always fulfilled, and exceptions may be more common than generally assumed. Most evidence for post-entrapment modifications of fluid inclusions comes from laboratory reequilibration experiments using synthetic and natural fluid inclusions in quartz. It has convincingly been demonstrated that fluid inclusions can stretch or shrink if large internal or external overpressures are applied (Pêcher 1981; Gratier and Jenatton 1984; Boullier et al. 1989; Sterner and Bodnar 1989; Vityk and Bodnar 1995), that they exchange hydrogen with the surrounding fluid (Mavrogenes and Bodnar 1994; Morgan *et al.* 1993), and that they can lose or gain H_2O in response to gradients in pressure and/or water fugacity (f_{H_2O}; Bakker and Jansen 1990, 1991, 1994; Qin et al. 1992; Hall and Sterner 1993; Sterner et al. 1995; Bakker and Diamond 1998). Field evidence in support of hydrogen diffusion and selective H_2O loss from fluid inclusions is given by studies of metamorphic terrains, for example from mineral assemblages that are incompatible with the fluid in contemporaneous fluid inclusions (Hollister 1990; Boullier et al. 1991; Johnson and Hollister 1995; Ridley and Hagemann 1998). Migration of fluid inclusions within quartz crystals has been described by Roedder (1971) and Swanenberg (1980), and migration of fluid inclusions in other minerals (ice, halite) by Hoekstra et al. (1965), Roedder and Belkin (1980) and Chou (1983).

Despite compelling evidence for open system behavior of fluid inclusions in some laboratory and field situations, the exact mechanism of material exchange is still largely unknown. Bulk diffusion through the quartz lattice may explain the experimentally produced changes in hydrogen fugacity (Mavrogenes and Bodnar 1994). In the case of H_2O however, the direction and rate of the

exchange often stands in marked contrast to what would be expected from simple f_{H_2O}-gradients, implying that different mechanisms may be operating as well. Stress-induced hydrolysis of lattice defects and microcracks has been proposed by several workers and could be an efficient way to remove H_2O from fluid inclusions (Bakker and Jansen 1994; Cordier et al. 1994). Because of the close relationship between this mechanism and bulk diffusion, careful experiments are needed to quantify their relative importance (Bakker and Diamond 1998). The mechanism of fluid inclusion migration is not well understood either. Roedder (1984) proposed that it may be due to heterogeneously distributed residual strain, which causes solubility gradients within the inclusions.

This paper reports several phenomena observed in natural quartz crystals, which together may help to resolve some of the questions addressed above. On a variety of diagnostic examples it is demonstrated that fluid inclusions are able to migrate over relatively large distances within their host, and that this process is associated with a change in inclusion volume, bulk density and fluid composition. However, not all phenomena are fully understood, and some of them could probably be explained in different ways. At first sight, the long list of various modifications may give the impression that fluid inclusions are generally unreliable records of their original volume and composition. However, a closer inspection reveals that most of these modifications can be recognized, which paves the way to differentiate between reliable and suspect fluid inclusions in other samples.

Observations

Most observations have been made on doubly polished thick sections of quartz crystals from the tin-mineralized Mole Granite (Eastern Australia), using a standard petrographic microscope. These crystals usually contain a core of dark and light colored smoky quartz, and an outer zone of clear to milky quartz. Sometimes, precipitation of other minerals is recorded at the interface between layers of contrasting color. Fluid inclusions are usually well preserved, but there are always some inclusions showing signs of post-entrapment modifications, such as partial decrepitation, migration away from original host planes, and unusual microthermometric behavior (see below). The sections varied between 200 μm and 500 μm in thickness and usually were prepared parallel to the c-axis of the crystals. As a complementary tool, LA-ICP-MS has been used to analyze the major and trace-element composition of individual fluid inclusions and the surrounding quartz. Other quartz crystals have been studied from base-metal deposits in Hungary and Chile, and from mineralized fissures ('Zerrklüfte') in the Swiss Alps (Table 1). Despite the fact that all phenomena will be reported from free-standing quartz crystals they are actually more common in massive vein quartz and phenocrysts. However, the petrographic situation in the latter samples often is too complex to draw any conclusions on the origin of these phenomena. Throughout this text, the sample names have been replaced by italic numbers (in brackets) which are given in Table 1.

Stress in free-standing quartz crystals

A key observation is the occurrence of fluid inclusion trails in tips of clear, euhedral quartz crystals which have grown into open spaces and therefore cannot have been affected by mechanical deformation (Fig. 1A). The fact that many of these cracks originate from former crystal surfaces and extend only a short distance into the crystal implies that the responsible stress was built up during growth and was highest on the crystal surface before it

Table 1. Description of the samples mentioned in the text

Sample	Locality	Mode of occurrence	Mineral paragenesis	Inferred formation temperature
Gulf (*1*) Leno (*2*) Boyd (*3*)	Mole Granite (Australia)	Free-standing crystals (1–4 cm) in miarolitic cavities	Quartz, orthoclase ± tourmaline (*2*), muscovite (*2*/*3*), topaz (*3*)	Core: > 500 °C Rim: ~200 °C
Emer5 (*4*) Uppw9 (*5*) Uppw*5 (*6*) Elliots (*7*) Sile18 (*8*)	Mole Granite (Australia)	Free-standing crystals (5–10 cm) from mineralized vein systems within the granite (*5*/*6*/*7*/*8*) or overlying sediments (*4*)	Quartz + wolframite (*4*/*5*/*6*/*7*) or cassiterite (*8*); ± beryl, fluorite, tourmaline, muscovite, adularia, arsenopyrite	Core: 500–600 °C Rim: < 200 °C
Cara1 (*9*)	Caracoles district (Chile)	Quartz crystals (1–2 cm) overgrowing massive ore in vein-type deposit	Quartz, pyrite, chalcopyrite	< 250 °C (?)
Lukm9b (*10*)	Lukmanier Pass (Swiss Alps)	Base of a free-standing crystal (4 cm) from an Alpine fissure	Quartz, albite and chlorite	> 320 °C
Nade1 (*11*)	Piz Nadéls (Swiss Alps)	Free-standing crystal (4 cm) in Alpine fissure	Quartz, albite, adularia	300–350 °C
Sche2 (*12*)	Schemnitz (Hungary)	Drusy quartz (3 cm) intergrown with ore in vein-type deposit	Quartz (amethyst), sphalerite, galena, chalcopyrite, pyrite	< 250 °C (?)

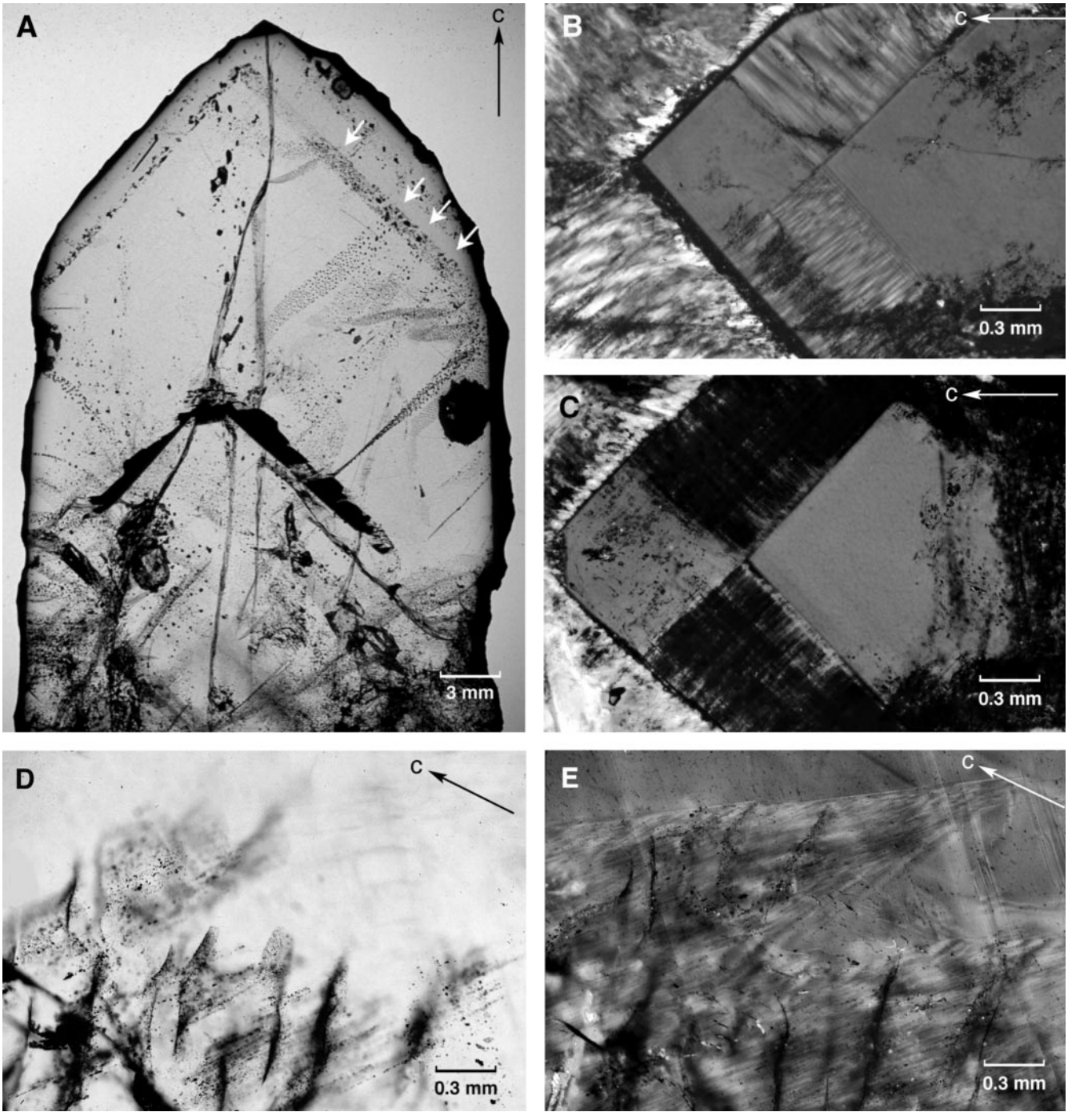

Fig. 1A Thick section of a zoned, free-standing quartz crystal from the Mole Granite (*3*), containing pseudosecondary trails of fluid inclusions which originate from a former crystal surface in the tip (*white arrows*). The c-axis orientation of the quartz is shown in the upper right corner of each image. **B** Quartz crystal showing an untwinned core (*right*) which is overgrown by later generations of optically more or less continuous, partially Brazil-twinned quartz (*9*). Note that the apical sector in the first overgrowth zone remained untwinned, and that the second zone starts with a short period of fibrous growth. Transmitted light and crossed polarizers (*X-pol*), with the sample rotated to near-complete extinction. **C** Similar crystal as in B, showing also an untwinned core, a first overgrowth zone of twinned quartz, and a later overgrowth zone starting with a period of fibrous growth. The twinned parts of the first overgrowth layer appear black due to the presence of innumerable small fluid inclusions, whereas the untwinned apical sector contains only relatively few inclusions (*9*) (*X-pol*). **D** Small fluid inclusions (*black dots*) spread out to both sides of original fracture planes, which are arrayed almost vertically in the image. The large original inclusions seem to have disintegrated into numerous smaller liquid- and solid inclusions during migration away from the fracture plane (*7*). **E** Same view as in D, but with the polarizers crossed to make Brazil twinning visible. The image shows that the pseudosecondary cracks formed only in the twinned areas, and that the migration direction of the fluid inclusions is parallel to the lamellae

was released by crack formation. The relationship between stress generation, the formation of cracks and post-entrapment modification of fluid inclusions is particularly well developed in crystals showing a characteristic, lamellar structure.

Significance of lamellar structures

In the studied thick sections, three different types of lamellar structures have been observed: twins, fibrous growth and deformation lamellae. One type is visible only in cross-polarized light, and is typical of outer parts of strongly zoned crystals. (Fig. 1B, C, E; Fig. 2B, C) (*4–9,12*). Close to complete extinction of the crystal, a characteristic pattern of weak interference colors appears, which is produced by optically slightly divergent lamellae following planes parallel or subparallel to $\{10\bar{1}1\}$ and $\{01\bar{1}1\}$ (rhombohedra r and z). These features often start at former growth surfaces which are marked by an abrupt color change or by the precipitation of other minerals, and extend approximately at right angles into younger quartz generations (Fig. 1B). In sections perpendicular to the c-axis of the crystals, it could be observed that the optical orientation of the lamellae is opposite to that of the host, implying that left-handed and right-handed quartz individuals are intergrown at these places. This feature is called 'Brazil'-twinning or 'optical' twinning, and is known to be exclusively a primary feature which forms as a result of rapid crystal growth and remains stable during mechanical deformation or heating above the α/β-transition at 573 °C (Hartley and Wilshaw 1973; Rykart 1989). Besides optical identification, the presence of Brazil twinning in the studied crystals has also been verified by etching with hydrofluoric acid.

An optically very similar feature, which often passes over into Brazil twinning, is fibrous growth. This phenomenon results from strong SiO_2-supersaturation in the fluid, which leads to spontaneous nucleation of small crystallites that tend to settle onto the crystal surface (left part of the crystals in Fig. 1B, C) (*9,10*). As a consequence, the crystal splits up into numerous subindividuals during further growth and returns only slowly – if ever – back to its original crystallographic orientation. It seems that a nearly continuous transition exists between such fibrous growth (which usually occurs parallel to the c-axis) and Brazil twinned growth.

A third type of planar structures resembles very fine cracks that follow planes parallel to r, z and the basal pinacoid c $\{0001\}$, and to a lesser degree to m $\{10\bar{1}0\}$. The crystallographic orientation and optical properties of these structures agree very well with lamellae produced during deformation experiments, as described by Twiss (1976), Blacic (1975) and Doukhan and Trépied (1985).

Of all these different types of lamellae, only Brazil twinning is of further importance for this article. This type of twinning has been observed in practically every crystal from the studied vein-type deposits ($n \approx 50$), but only in about 50% of the samples from Alpine fissures ($n \approx 20$), and in no crystal from miarolitic cavities ($n \approx 15$). The following observations show that Brazil-twinned growth is closely related to the formation of fluid inclusions and to their subsequent modification.

1. Primary fluid inclusions are preferentially trapped in Brazil-twinned quartz (*7–9,12*). This is particularly well visible in the crystal of Fig. 1C, in which the twinned sectors contain so many inclusions that they appear black, whereas the untwinned areas remained nearly inclusion-free.

2. Brazil twinning has a strong influence on the generation of pseudosecondary and secondary fluid inclusions, too (*7,12*). This is demonstrated in Fig. 1D, E, which shows pseudosecondary trails of fluid inclusions occurring only in the Brazil-twinned areas. As Brazil twinning is known to be a *primary* feature, and crack formation always is a *secondary* process, the cracks must have formed as a result of the twinning – and not vice versa. This shows that Brazil twinned growth can produce stress which is high enough to result in partial failure of the crystal.

3. The same stress apparently forces individual fluid inclusions to migrate along twin boundaries away from their original position on the host plane (Fig. 1D, E) (*4,7–9,12*), a process which often is associated with the formation of secondary fluid inclusions and solid inclusions on their way. Fig. 2A, B show a fluid inclusion trail cutting across a zoned crystal with an untwinned center and a strongly twinned rim. In the untwinned (and therefore stress-free) center, the fluid inclusions stayed more or less on the trail, whereas in the twinned outer regions they have migrated away from it by following the respective orientation of the twin lamellae.

In these examples, the formation of fluid inclusions and their later modification is apparently related to Brazil twinning. However, in the next chapter it will be shown that similar results can be produced also by other mechanisms.

Stress in lamella-free crystals

Brazil twinning cannot be the only reason for the generation of internal stress in free-standing quartz crystals, as cracks are common also in tips of optically untwinned crystals. Other evidence is found in examples like the one in Fig. 2C, implying that the disintegration of fluid inclusion trails was independent of the occurrence of Brazil twinning: the trail portions in the untwinned area in the right part of the figure display the same amount of deformation as the other portions in the twinned area on the left. The similar orientation of the lamellae and the direction of migration of the fluid inclusions seems to be rather accidental in this case, as in other parts of the same crystal these features are orientated at a high angle to each other. The mechanisms leading to the generation of stress in untwinned crystals will be discussed later.

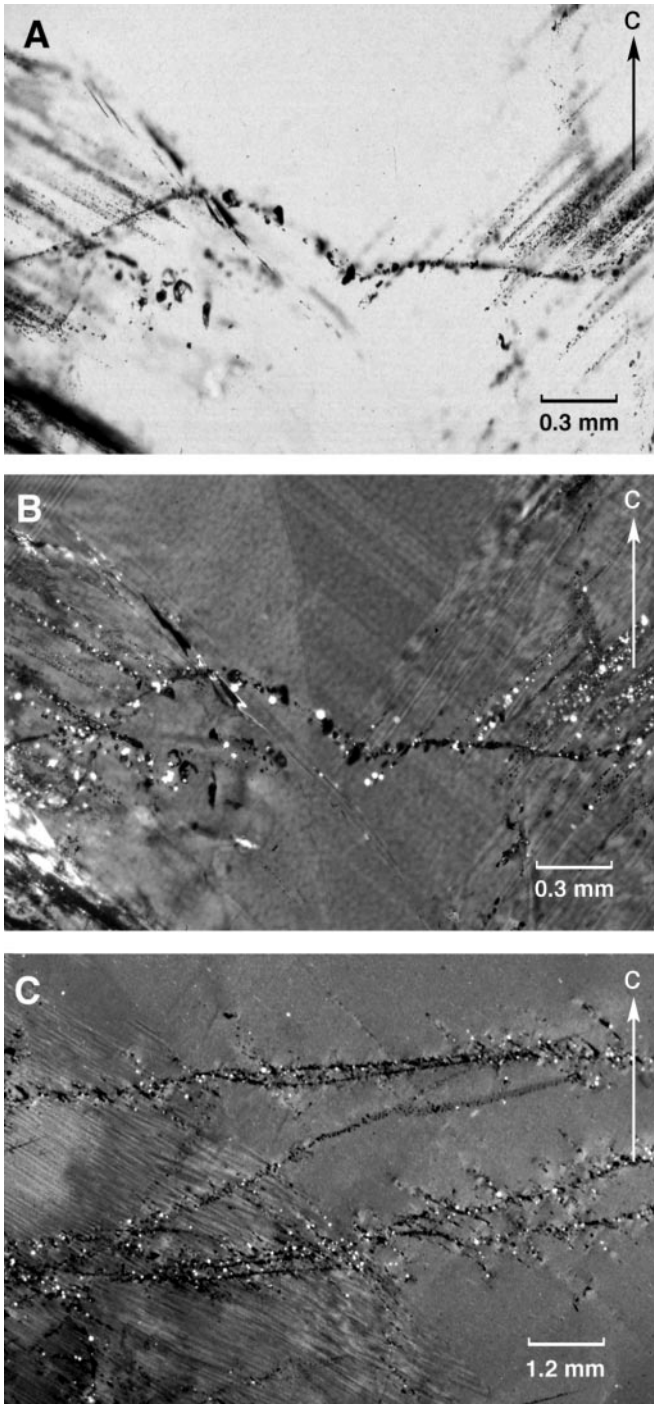

Fig. 2A Pseudosecondary fluid inclusions (trail is approximately horizontal in the figure), which have remained unmobilized in the center, but are strongly dispersed in the outer zones of the crystal (*12*). **B** Same field of view as in A, but now photographed with crossed polarizers. The fluid inclusions obviously migrated away from the fracture plane only in the Brazil-twinned domains, and thereby followed the twin boundaries. Minerals that formed behind (or were abandoned by) the migrating inclusions appear as *white dots* (*X-pol*). **C** An example of trail disintegration that is independent of the occurrence of Brazil twinning (see text; *X-pol*) (*5*)

Modification of fluid inclusions

Of the many reasons for post-entrapment fluid inclusion modifications mentioned in the introduction, those related to deformation processes seem to play the dominant role in the quartz crystals examined during this study. However, other geological settings may exist in which the other mechanisms might become dominant. Most of the observations presented below will later be used when discussing reasons for migration and H_2O loss from fluid inclusions.

1. There are two different ways by which fluid inclusions can "migrate" away from their original position on a fracture plane or a growth zone. One possibility is the generation of small cracks, into which the fluid from already existing inclusions is expelled, thereby forming secondary inclusions (*4,5*). The other possibility is the migration of inclusions *as a whole* by continuous dissolution and re-precipitation of the surrounding quartz. Fluid inclusions interpreted to have moved by this second mechanism often left smaller residual inclusions (solid or liquid) behind on their way (Fig. 3A). From here on, the term 'migration' is used only for the movement of whole inclusions.

2. Residual solid inclusions behind migrated fluid inclusions often resemble abandoned daughter minerals, which would imply that considerable cooling had occurred before the onset of migration. However, on trails which are only partly disintegrated it can be observed that the sum of all these "abandoned daughter minerals" is far higher than the amount of daughter minerals in the immobilized inclusions (*2,3,5,8*). At least in these cases it seems that the solids are minerals that formed by re-precipitation of dissolved SiO_2 together with other fluid components such as Na, K, Al, etc.

3. Deformed fluid inclusions commonly are surrounded by a halo of very small secondary inclusions occurring in planes parallel to the c-axis of the crystal (Fig. 3C, D) (*2,4,10,11*). In cases where these "sweat haloes" are separated from the main inclusion by clear quartz, they seem to outline a former contour of the fluid inclusion (Fig. 3B–E). This implies that the inclusion was once much more flattened and elongated, before it recrystallized back to a more equant shape. The volume between this new shape and the former fluid inclusion contour is thereby filled with clear quartz. Usually, two sets of halo-cracks were developed at nearly a right angle to each other, with one large crack extending symmetrically from both ends of the inclusion, and two smaller cracks extending either above or below this plane (Fig. 3B, C and Fig. 4). From this observation it can be concluded that the stress was asymmetrically distributed around the inclusion, and hence was not produced by overpressure within them. This stands in marked contrast to fractures around quartz-hosted melt inclusions (Roedder 1984) and radioactive minerals (zircon, thorite), which do not show

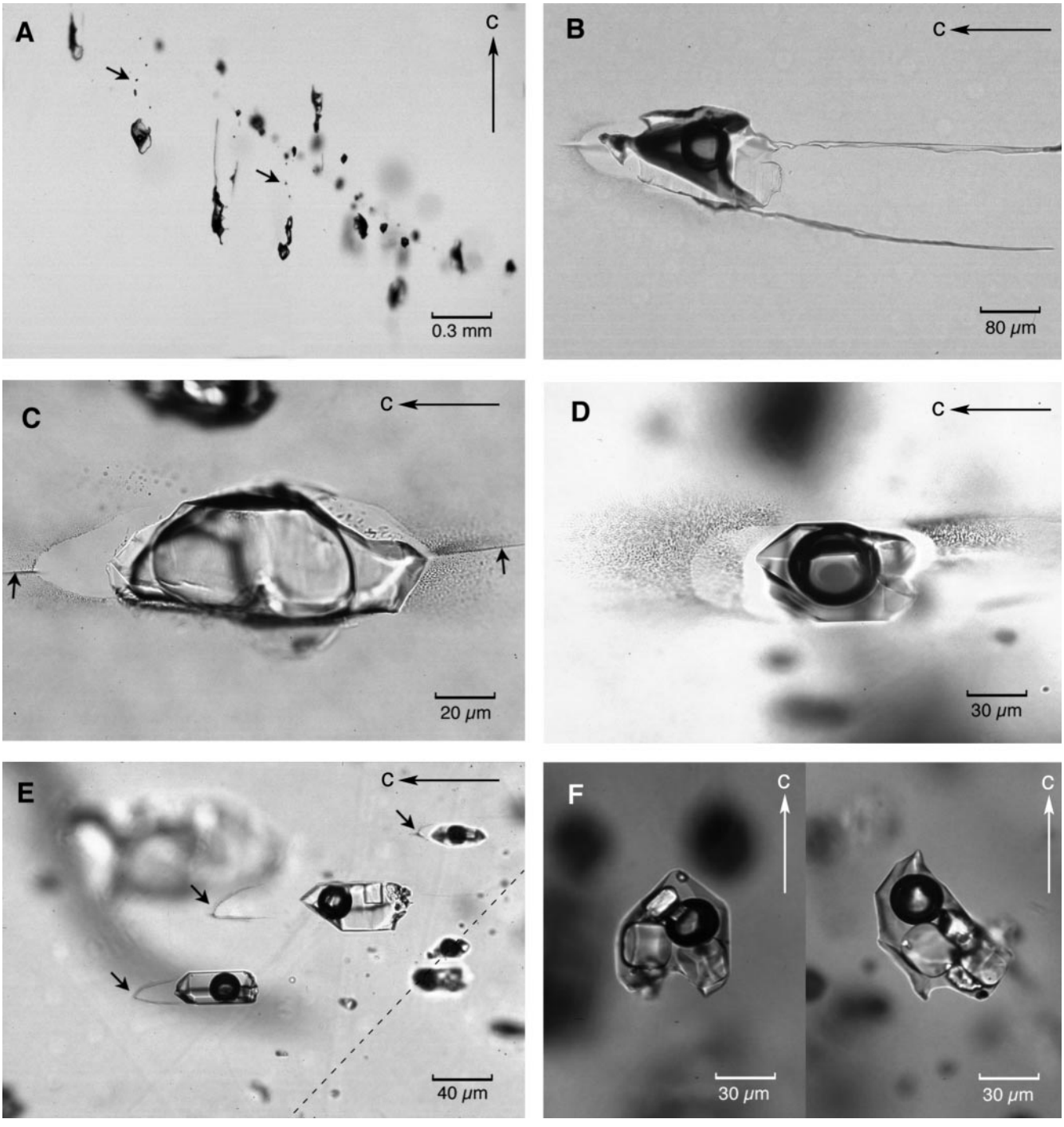

Fig. 3A Fluid inclusion trail that has been affected by deformation (*11*). Some inclusions migrated considerable distances away from the original plane extending diagonally from the upper left to the lower right. The larger inclusions migrated away in both directions from this plane and left tails of residual fluid- and solid inclusions (*arrows*) behind, whereas smaller inclusions remained mainly immobile. **B** Close view of a fluid inclusion that belongs to the same trail as in A, and that has migrated away from it towards the left (note c-axis orientation). During migration, the inclusion developed a weak sweat halo at its front, and formed two characteristic tails at its back. A small crack extends nearly vertically from the main sweat halo (in focus) into the area below. The inclusion is terminated by a flat surface in the focus plane, and extend into the third dimension only below this level. **C** CO_2-rich fluid inclusion from the Swiss Alps (*10*), showing a typical "sweat halo" developed in two planes which are nearly perpendicular to each other and parallel to the c-axis of the crystal, the larger plane being within the level of focus. The distribution of the haloes suggests that the inclusion once occupied a larger area, and then recrystallized back to a more equant shape. Of the two cracks (*arrows*) belonging to the subordinate fracture plane, one extends only above the level of focus, and the other only below it (cf. Fig. 4). **D** Example of a fluid inclusion with a multiple "sweat halo" (on its left), indicating that stress was maintained over a certain time (*4*). **E** Fluid inclusions that have migrated away from the original plane (dashed line) and have developed sweat halos (*arrows*) at their front (*4*). **F** Non-equilibrium shapes of fluid inclusions which have moved within the host quartz and are likely to have lost water. Note the characteristic reentrants (*2*) (*X-pol*)

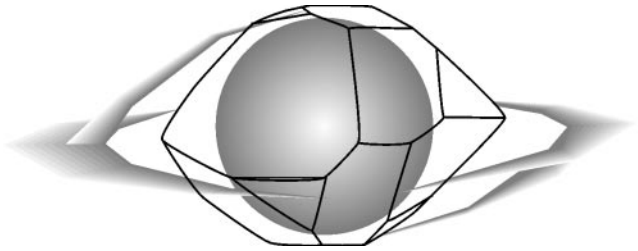

Fig. 4 Schematic view of a fluid inclusion that developed an asymmetrical sweat halo in two perpendicular planes parallel to the c-axis

this systematically asymmetric arrangement. The same conclusion can be drawn from the fact that the micro-inclusions in the sweat haloes show variable filling ratios, implying that the fluid in the main inclusion was heterogeneous at the time of crack formation, and hence was at lower pressure than at trapping conditions (*4*).

4. Fluid inclusions that moved away from the plane often display a well-developed sweat halo in their front and a weaker halo in their back, which – together with other fluid portions and solid inclusions – often can be traced back to the former position on the trail (Fig. 3B, E) (*4,10,11*). This observation and the occurrence of multiple sweat halos (each accompanied by a crack of the subset), demonstrates that the halo- and crack-formation was a repetitive process during the course of migration (*4,10*). In optically untwinned quartz, the migration always occurred parallel to the c-axis of the crystal, with about equal numbers of inclusions migrating upwards or downwards. Strongly deformed inclusions are flattened within the dominant crack plane and extend into the third dimension only towards the side on which the crack of the subset is developed (Fig. 3B) (*4,10,11*). Potential migration is more difficult to recognize in cases where the inclusions later recrystallized to more equant shapes, and do not show haloes or tails of secondary fluid- and solid inclusions any more. However, such inclusions can still be identified by their characteristic reentrants, which form as a result of recrystallization from an originally more irregular shape (Fig. 3D, F, and to a lesser degree 3E) (*1–4,6*).

5. If intact trails and disintegrated trails intersect each other, the latter always belong to the older generation. This has been verified on a large number of crosscutting relationships which all showed that migrated or deformed inclusions were refilled at the intersection with the fluid of the crosscutting, undeformed trail (*2,10*). The stress causing the modification of the older generation of fluid inclusions apparently was released before the formation of the second generation, as the latter shows no signs of deformation.

6. Many fluid inclusion trails in the quartz crystals from the Mole Granite (*1–4*) show unambiguous assemblages of brine and vapor inclusions that were trapped from a boiling hydrothermal fluid (Fig. 5) (''boiling assemblages''; see also Audétat et al. 1998). In some of these boiling assemblages the brine inclusions systematically homogenize by halite dissolution (*2*) (Fig. 5B, C). However, any inclusion formed under these conditions should actually homogenize by bubble or liquid disappearance (end-members at the temperature of formation). The presence of a salt crystal above their liquid-vapor homogenization can be explained by a post-entrapment increase in density (volume reduction), a selective loss of H_2O (increase in salinity), or a combination of these two processes. Theoretically it could also be the result of accidental trapping of halite crystals, but the relative uniformity of halite melting temperatures (Fig. 5B) and the absence of solid halite inclusions in the quartz render this explanation very unlikely. Similar boiling assemblages have been observed also in high-temperature quartz veins from a Cu-Au-porphyry in Argentina (T. Ulrich, personal communication). It is disconcerting that the volumetric and/or compositional modification was noticed only because of this physical contradiction, as the trails otherwise show no textural evidence for any disturbance (such as shape deformation and/or displacement).

7. In some boiling assemblages it can be observed that large brine inclusions have migrated considerable distances away from the trail, whereas vapor inclusions and smaller brine inclusions remained immobile (*2*). Large mobilized brine inclusions have a markedly higher salinity and density than those remaining on the plane (Fig. 5C; Table 2). This salinity increase is expressed by a change from homogenization via bubble disappearance to homogenization via halite dissolution. Four conclusions can be drawn from these observations:

1. Brine inclusions are more susceptible to migration than vapor inclusions of equal size.
2. Large inclusions are more easily mobilized than small inclusions.
3. Migration is associated with selective loss of H_2O.
4. Migration leads to decreasing inclusion volume and increasing filling ratio (i.e. increasing bulk density).

8. Two pseudosecondary trails with no signs of mobilization display another very unusual phenomenon (*2*): inclusions close to the original crystal surface have a lower density, but higher salinity than inclusions along the same trail further inside the crystal (Fig. 5A). Any trend produced by fluid mixing, heterogeneous trapping from a boiling fluid or necking down would result in a *positive* correlation between salinity and density. The only explanation for this is loss (or gain) of water.

LA-ICP-MS analyses

Laser-ablation inductively-coupled-plasma mass-spectrometric microanalysis of quartz and contained fluid inclusions was used to explore the following two questions: (a) is only H_2O removed from the fluid inclusions, or does the post-entrapment modification selectively alter any solute ratios? (b) to what degree does textural or color zonation in quartz crystals reflect the trace-element composition of quartz? All measurements were performed using a LA-ICP-MS system that has been designed and optimized

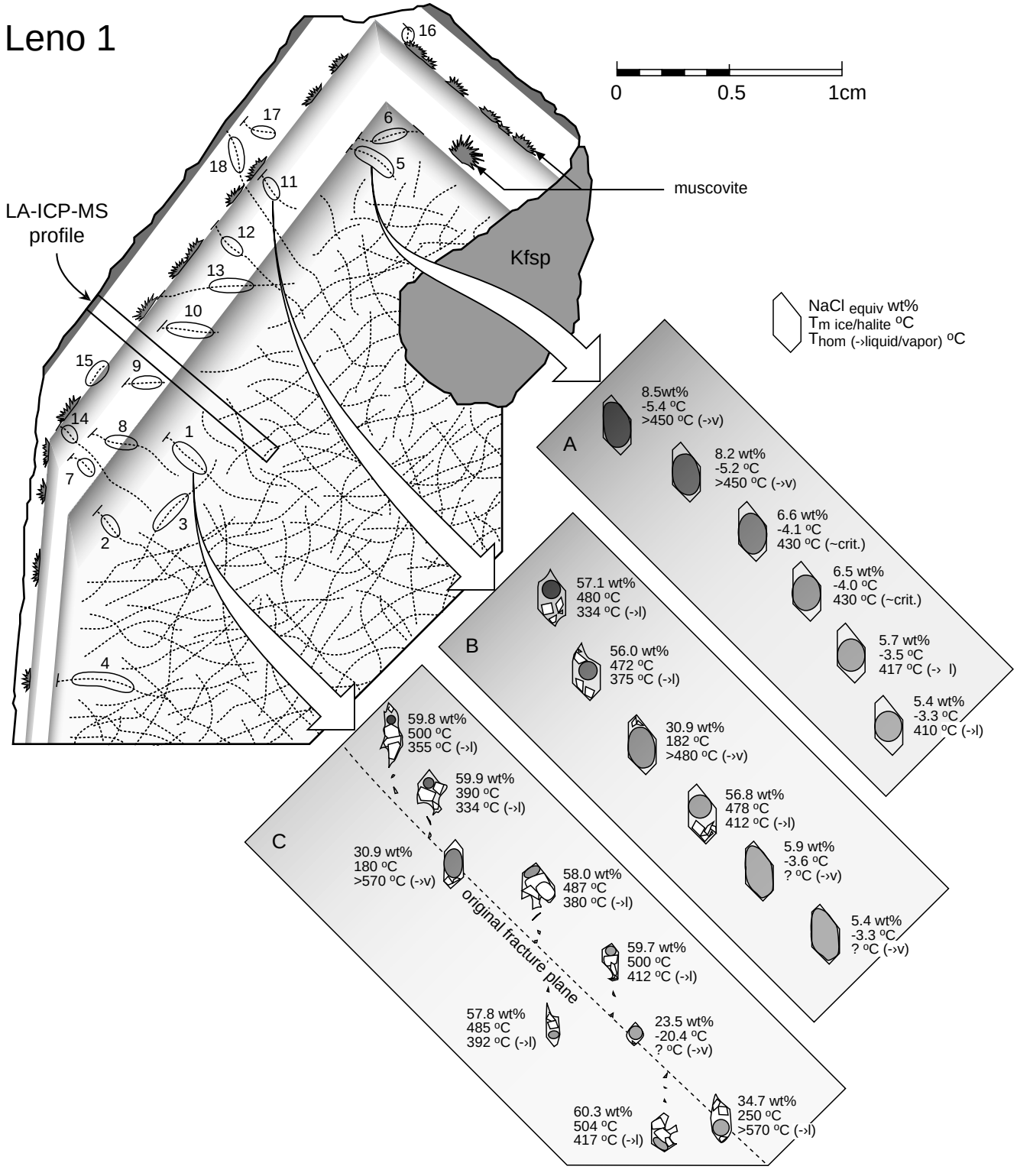

especially for fluid inclusion analysis (Audétat et al. 1998; Günther et al. 1998). The system consists of an ArF Excimer laser (193 nm; Compex 1101, Lambda Physik, Germany) that is combined with a modified quadrupole mass spectrometer (Elan 6000, Perkin-Elmer, Canada). The laser beam with a flat-top beam profile is imaged onto the sample surface by mirror optics in a petrographic microscope, which allows the sample to be observed during ablation. This, and the possibility to switch instantaneously between different beam spot diameters (4, 10, 20, 40, 60 and 80 μm) are two prerequisites for accurate fluid inclusion analysis. The use of a modified ICP-interface and mixed Ar/He-gas as transport medium enables measurements with high sensitivity and low background, and the simultaneous detection of up to 40 major and trace elements as transient signals. A more complete description of the system and its use for fluid inclusion analysis can be found in Günther et al. (1998).

◀

Fig. 5 Cross-section through a zoned quartz crystal from a miarolitic cavity of the Mole Granite (*2*). The trails in the core of the crystal are generally more affected by deformation than the trails close to the surface. Inset *A* shows a trail with a very uncommon salinity/density-trend, which can be produced only by a loss (or gain) of water. Trail *B* is petrographically a clear boiling assemblage, but the brine inclusions homogenize by halite dissolution, which theoretically is impossible (see text). Trail *C* is a typical example of a deformed boiling assemblage, showing vapor inclusions and intermediate members that remained on the original fracture plane, whereas most brine inclusions have migrated away from it and left newly formed (or abandoned) minerals behind. The water loss from the brine inclusions is reflected in their homogenization mode, which changes from "homogenization by bubble disappearance" in those remaining on the plane (lowermost inclusion), to "homogenization by halite dissolution" in the migrated ones. The numbering of the trails reflects their relative age, which is inferred from their petrographic position (*small lines* designating their starting point on the former crystal surface) and few crosscutting relationships. This temporal classification will later be used for the reconstruction of the chemical and physical (p/T) evolution of the fluid (Fig. 7), and to relate it with the trace element composition of the quartz determined along the LA-ICP-MS profile

Compositional changes in migrating fluid inclusions

The possibility that solute components were selectively removed from migrating fluid inclusions was tested on a single trail displaying the same features as described in observation 7 of the previous section. In this trail, the salinity of the brine inclusions increases from 34 wt% $NaCl_{equiv}$ in the unmobilized inclusions to a maximum of 58 wt% $NaCl_{equiv}$ in the migrated ones, which corresponds to a H_2O loss of up to 46% assuming that the unmobilized inclusions have retained their original salinity (Table 2). A comparison of their composition (Fig. 6) shows that most element ratios remained unmodified, except for Li which was lost during migration. The latter is readily explained by the incorporation of Li into the quartz lattice (see below). Considering the fact that several solid phases were formed (or left) behind the migrated fluid inclusions it is surprising that the element *ratios* remained so constant. It implies that – at least in this particular case – the formation of minerals had little effect on the relative element concentrations in the fluid inclusions, and that only H_2O and Li were lost in substantial amounts.

Trace element composition of quartz

LA-ICP-MS was also used to measure the trace element content of quartz across the strongly color-zoned profile marked in Fig. 5. The results are plotted in Fig. 7 where they are spatially/temporally correlated with quartz coloration, fluid composition and the inferred crystallization temperature. The fluid composition and quartz crystallization temperature could be reconstructed from microthermometric measurements and LA-ICP-MS analyses performed on various generations of pseudosecondary fluid inclusions, which age relative to the growing crystal could be assessed on the basis of petrographic criteria (Fig. 5). The crystallization tempera-

Table 2 Microthermometric data and LA-ICP-MS results from unmobilized (top 6) and mobilized (bottom 5) brine inclusions on a trail similar to that in Fig. 5C. Numbers in *italic* have not been considered for the average plotted in Fig. 6 (Sample: Leno 3.1)

Inclusion	Displacement (μm)	Filling ratio[2]	Tm_{halite} (°C)	Th-l (°C)	$NaCl_{equiv}$[3] (wt%)	Li (ppm)	K (ppm)	Mn (ppm)	Fe (ppm)	Zn (ppm)	As (ppm)	Rb (ppm)	Cs (ppm)	W (ppm)	Pb (ppm)
3	None	0.75	245	438	34.3	1457	65 080	31 084	98 071	9589	n.d.	2376	2542	120	4780
4	None	0.75	243	485	34.2	1352	63 656	33 608	110 069	9992	n.d.	2103	2256	100	4585
5[1]	None	0.75	245	490	34.4	1578	62 780	32 266	104 690	9085	n.d.	*1684*	*1873*	123	3944
8	None	0.75	247	> 500	34.5	1234	60 381	31 517	105 345	9907	n.d.	1889	2145	119	4334
12	None	0.75	248	457	34.6	1473	64 814	32 147	109 839	9297	n.d.	2200	2439	101	4449
13[1]	40	0.75	242	497	34.2	1682	*56 969*	*28 653*	105 134	*7221*	221	2127	2385	121	4504
15	120	0.90	482	394	57.3	451	128 739	53 446	193 622	14 997	762	5346	4970	*200*	10 297
16	80	0.90	493	367	58.8	459	117 159	59 274	200 826	12 995	633	5422	4809	329	9107
18	100	0.90	483	384	57.5	489	109 511	52 816	*149 198*	13 855	642	4930	*3861*	291	8805
19	70	0.90	378	354	45.1	*1056*	*67 182*	53 624	183 987	13 853	610	*4784*	4370	263	8213
20	70	0.90	491	358	58.8	573	121 620	58 427	202 003	15 811	685	5326	4795	303	9311

[1] Slightly decrepitated during ablation; may have lost parts of daughter minerals
[2] Corresponds to fraction of inclusion volume filled with liquid + crystals
[3] Calculated after Bodnar and Vityk (1994)

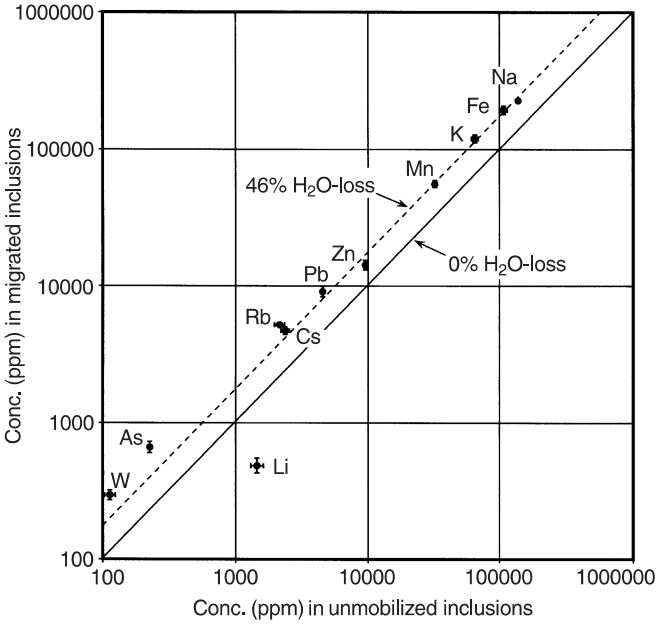

Fig. 6 Comparison of element concentrations in mobilized and unmobilized brine inclusions. Except for Li, which is incorporated into the host quartz, no components other than H_2O seem to have been removed during migration. The very small, but consistent differences in As and W are probably due to preferential loss of the other elements during the formation of the observed solids

tures plotted in Fig. 7D correspond to the final homogenization temperatures of the least modified inclusions. No pressure correction is needed because boiling assemblages occur in the whole temperature range.

The composition of quartz along the analyzed profile shows a clear dependence on the color distribution, with high concentrations of Al and Li occurring in the colorless zones, and lower concentrations occurring in the smoky layers. According to Rykart (1989) and Cohen (1989), the formation of smoky color centers in quartz is caused by a substitution of $[SiO_4]^{4-}$-tetrahedra by $[AlO_4]^{5-}$-tetrahedra in the same lattice configuration. The negative charge excess is compensated by small cations such as Li^+, Na^+ and H^+ which fit into neighboring lattice interstices. A second precondition for smoky coloration is the dominance of $(Li^+ + Na^+)$ over H^+ (Rykart 1989). As colorless layers in the analyzed profile contain more Al, Li, Na and Sb than smoky layers their lack in color centers are likely to be due to an excess of H^+ over $(Li^+ + Na^+)$.

The amount of trace elements incorporated into a quartz crystal mainly depends on its growth rate, the crystallization temperature, and the composition of the fluid (Martin et al. 1982; Wilke and Bohm 1988). The fact that the Sn- and Ti-concentration along the analyzed profile follows a trend very different from that of Li, Na and Al demonstrates that several of these factors must have played a role. The effect of fluid composition on color zoning probably was minor, as the Li-concentration in the fluid drops by more than an order of

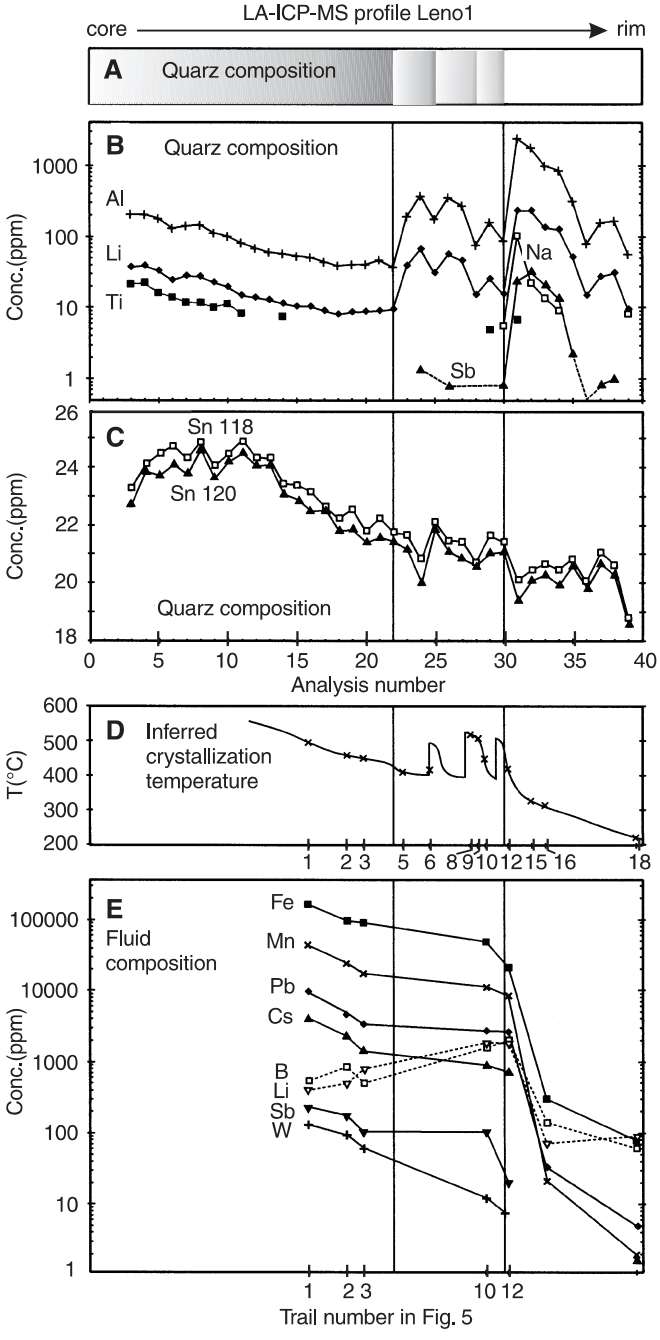

Fig. 7 A–E Spatial correlation of the quartz coloration **A** along the profile marked in Fig. 5, with LA-ICP-MS analyses of the quartz (**B**+**C**), inferred crystallization temperature (**D**) and LA-ICP-MS analysis of contemporary brine inclusions (**E**). The colorless quartz layers contain higher amounts of trace elements than the smoky layers, which probably is due to faster growth rates. Exceptions are found in Sn and Ti which do not show this dependence. The compositional evolution of the contemporaneous fluid reflects mixing of a magmatic brine with meteoric water that was enriched in B and Li due to the condensation of B- and Li-rich magmatic vapor into it. Sn and Ti could not be measured in the fluid inclusions because of relatively high background values (Sn) and low concentrations in the fluid (Ti). Sn is also susceptible to interference problems by other elements, whose occurrence can be ruled out if the measurements on two separate isotopes give the same result (Fig. 7C)

magnitude at the same time as the Li-concentration in the quartz increases by an even bigger factor. The lack of a correlation between fluid temperature and the abundance of Al, Li, Na and Sb in the quartz leaves crystal growth rate as the dominant factor controlling the incorporation of these elements. Ti and Sn on the other hand seem to be controlled at least partly by temperature. This is indicated in the outer zones of the crystal, where temperature drops are associated with decreasing concentrations of Sn in the quartz, but increasing concentrations of Al, Li, Na and Sb due to the faster crystallization rates. Together with the information on fluid composition (Fig. 7B) and studies on other crystals from the Mole Granite (Audétat et al. 1998) the following crystallization history can be reconstructed for the sample shown in Fig. 5. In a first stage, quartz was precipitated at high temperature and at near-equilibrium conditions from a slowly cooling magmatic fluid within a miarolitic cavity. After this, several batches of hot magmatic fluid, which were increasingly diluted by meteoric water, seem to have passed through the cavity. Relatively rapid temperature drops resulted in faster growth rates and therefore larger amounts of H^+, Al^{3+}, Li^+, Na^+, Sb^{3+} incorporated into the crystal lattice. Temperature increases were generally not recorded because they are associated with quartz dissolution rather than quartz precipitation. Finally, the cavity was filled with cooler, meteoric groundwater. This event is not only recorded in the drastic change in the trace-element content of the quartz, but also in the precipitation of muscovite onto the crystal surface. At temperatures below 200 °C, crystal growth became insignificant.

Discussion

Causes of stress in quartz crystals

Stress in vein quartz, phenocrysts and bases of free-standing crystals is mainly the result of mechanical deformation. However, cracks originating from former surfaces of free-standing crystals must have been generated by a different mechanism. It has been shown that Brazil-twinned growth lead to the generation of stress in the twinned crystal domains, but there is abundant evidence that similar stresses occurred also in untwinned domains. These stresses must have been operating over long periods of time, as they allowed fluid inclusions to migrate over large distances within the host. The large number of cracks originating from conspicuous growth zones further indicates that stress was increasing towards the crystal surface and probably was caused by the same process that lead to the compositional zonation. This stress could either be generated by the growth process itself (as in the case of Brazil twinning) or by the effect of cooling. For example, high surface tensions can temporarily be produced in a homogeneous material by rapid cooling (quenching). However, it is very unlikely that the features shown in Fig. 5 result from this mechanism, as the fluid temperature in a miarolitic cavity is very unlikely to drop so rapidly that significant temperature gradients can build up within a crystal, and because the resulting stress would last only as long as the crystal is out of thermal equilibrium. This time-period is certainly too short to enable fluid inclusions to migrate over large distances within the host. An experiment on clear, inclusion-free quartz crystals from Alpine fissures has shown that about 50 °C quenching within one second is necessary to produce cracks on their surfaces – a temperature-drop which is very unlikely to occur within a miarolitic cavity. Therefore, at least in the crystals from miarolitic cavities the stress must have been generated by the growth process itself.

In the synthetic quartz production industry it is well known that crystals may crack spontaneously, or fail under a weak load. The high stress within these crystals is generated by a large density of lattice defects, such as screw dislocations, edge dislocations and subgrain boundaries (Yoshimura et al. 1979, Wilke and Bohm 1988). These lattice defects result either from rapid crystal growth, from disturbances in the form of fluid- or solid inclusions, or from changes in the quartz composition (Spencer and Haruta 1966, Wilke and Bohm 1988). In the latter case, already small differences in trace element composition of quartz can lead to relatively large stresses within the crystal. Yoshimura et al. (1979) showed that massive lattice disturbances in synthetic quartz have been generated because of only 20 ppm (by weight) difference in the (Al + Na)-content above different growth faces, which was associated with a 0.0015% increase in the lattice parameters. This agrees relatively well with values given in Rykart (1989), showing that the incorporation of 500 ppm (Li + Al) is associated with an increase in the a_o lattice parameter (4.9130 Å) by 0.0008 Å (+0.016%).

A very impressive example is given by Sheftal and Gavrilova (1966), who observed that thick seed plates of synthetic, colorless quartz developed cracks as soon as smoky quartz was grown onto them. These cracks formed at a right angle to the crystal surface and are believed to be caused by the 0.0005 ± 0.00015 Å increase in the lattice parameter, which would correspond to about 800 ppm difference in Li + A1 based on the values of Rykart (1989).

These two examples demonstrate that even without changes in temperature or pressure it is possible to generate high stress within quartz crystals. Compared to artificially grown crystals, the growth conditions of natural samples were much more chaotic, involving large variations in the fluid temperature, fluid composition and growth velocity, as well as trapping of fluid- and solid inclusions. Accordingly, the observed variation in trace elements is much larger (up to 2000 ppm Li; Fig. 7E), and the resulting stresses are therefore clearly

adequate to produce fractures and stress-induced fluid inclusion migration.

Migration and H_2O loss from fluid inclusions

There is considerable dispute about the mechanism of H_2O loss from fluid inclusions. Strain-enhanced leakage is proposed by Hollister (1990), Bakker and Jansen (1991, 1994) and Johnson and Hollister (1995), whereas bulk diffusion is preferred by Cordier et al. (1994). According to the first model, strain is caused either by overpressure in the inclusions or by mechanical deformation, and leads to the nucleation of dislocation loops. Both the generation of dislocation loops and their expansion along definite planes within the crystal needs H_2O to break the Si-O-bonds. Such a mechanism is indicated by TEM-images showing that small water-bubbles formed during heat treatment of experimentally deformed quartz crystals (Bakker and Jansen 1991, 1994). Vityk (1998) reports similar bubbles in dislocations that formed around experimentally overpressured fluid inclusions. Bakker and Jansen (1991, 1994) argued that the solubility and bulk diffusivity of water-related point-defects, as reviewed by FitzGerald (1991), is too slow to account for the H_2O loss observed in their experiments, and concluded that water migrated out in molecular form along dislocations and planar defects. However, based on a quantitative reappraisal of different leaking mechanisms, Cordier et al. (1994) proposed that bulk diffusion has the larger impact over geological time scales.

In this work, the close relationship between migration and H_2O loss from fluid inclusions clearly supports the model of strain-enhanced leakage. The presence of optically visible water bubbles on distinct planes (''sweat haloes'') around fluid inclusions indicates that stress resulted not only in individual dislocation loops (as in the experiments of Bakker and Jansen 1991), but in the formation of entire dislocation planes. The asymmetric stress-field within the quartz crystals produced two sets of haloes, of which one usually is more strongly developed than the other (observation 4). The steady supply of H_2O from the fluid inclusions allowed further breaking of Si-O bonds, and therefore a continuous propagation of these cracks. Any crack that forms around a fluid inclusion strongly increases its surface energy, which the inclusion immediately starts to reduce by recrystallizing into a new shape. As the surface free energy on the crack plane is higher than on the negative-crystal faces, quartz will be dissolved mainly in the region of the crack and be re-deposited on the other faces. As soon as fresh, unstressed quartz is deposited on these faces, the already existing solubility gradient within the inclusion is intensified because the occurrence of stressed (and therefore more soluble) quartz is now limited to the vicinity of the crack. As a consequence, quartz will continue to dissolve there, and the inclusion will start to move along the slowly propagating crack. During migration, the inclusion attains an increasingly flattened and elongated shape, and sometimes leaves secondary fluid inclusions and solid inclusions behind (Fig. 3B). Once the stress is released, the crack stops propagating and the fluid inclusion has more time to recrystallize. To obtain the shape of a regular negative crystal it will dissolve quartz mainly on its sides and re-deposit it within the flattened extremities, resulting in a clear zone between the inclusions and their sweat haloes. Many of these features seem to disappear during later recrystallization processes.

From the close relationship between water-loss and fluid inclusion migration one could conclude that the missing water was incorporated into re-precipitated quartz behind the inclusions. However, this interpretation is compromised by the observation that water was lost also from unmobilized inclusions (observation 6), and by the following calculation: assuming that the host quartz was water-free and the re-precipitated quartz was very ''wet'' with 1000 $H/10^6$ Si atoms (Rykart 1989), the inclusions of Table 1 would have had to travel more than 200 times further to lose the observed 46% water.

Fluid inclusion migration in Brazil-twinned quartz probably was driven by a different process, as no cracks or sweat haloes can be observed along the twin boundaries. Because the fluid inclusions in twinned domains usually are very small, these features might be not visible, but it is also possible that the inclusions followed the twin planes simply because the quartz was more soluble along the twin-plane boundaries.

Conclusions

Post-entrapment modifications of fluid inclusions in natural quartz crystals are mainly the result of deformation processes, and hence are more common in vein quartz and phenocrysts than in free-standing quartz crystals. However, there is abundant evidence that deformation can occur also in free-standing quartz crystals, leading to a whole list of inclusion modifications such as changes in shape and composition, and migration within the host quartz. The cause of deformation in free-standing crystals is internal stress that builds up during rapid growth, Brazil twinning and/or compositional zonation. It has been shown that even small differences in the trace element composition of quartz can lead to stress high enough to induce cracking of a crystal and generation of fluid inclusion trails. On a smaller scale this stress is responsible for the generation of very fine cracks around individual fluid inclusions, which results in the formation of ''sweat haloes''. The continuous propagation of these cracks forces the inclusions to migrate within the host. This process is associated with a significant loss of H_2O (up to 50%) and Li from the inclusions, the latter apparently being incorporated into the crystal lattice. All other elements remain in basically unchanged concentration ratios within the migrating inclusions as long as no minerals are formed behind.

Despite the large number of modifications described in this article it would be wrong to conclude that fluid inclusions in natural quartz are generally unreliable records of original fluid properties, as the altered inclusions generally can be recognized. The main implications for fluid inclusion petrography are the following:

1. Isolated fluid inclusions in high temperature quartz veins and phenocrysts, which commonly are considered as primary, may in fact be secondary or pseudosecondary inclusions that have migrated away from the healed fracture planes.
2. Inclusions in crystals with strong chemical zonation, which may be evident from color distribution and/or textural criteria, are more likely to be affected by post-entrapment modifications than inclusions in chemically unzoned crystals.
3. Modification of fluid inclusions in response to quartz deformation can result in water-*loss*, but never in water-*gain* because the deformation process *consumes* H_2O. Measured fluid salinities might therefore be too high, but never too low.

The likelihood of H_2O loss is indicated by the following petrographic and microthermometric features:

1. Fluid inclusions with "sweat halos".
2. Small solid inclusions that resemble daughter minerals and occur in lines behind isolated fluid inclusions.
3. High temperature fluid inclusions with outlines that strongly deviate from minimum surface energy (re-entrants in negative-crystal shape; e.g., Fig. 3F).
4. Occurrence of Brazil twin lamellae, visible in cross-polarized light.
5. A relatively large spread in microthermometric data, which cannot be explained by heterogeneous trapping or necking down.
6. Clear-cut boiling assemblages containing brine inclusions that homogenize by halite dissolution.
7. Variations in fluid density and/or salinity in fluid inclusions along a single trail; in particular, trends towards lower density but higher salinity.

In summary, it is proposed that careful petrographic and microthermometric study of fluid inclusion populations generally permits recognition of those inclusions that do not match the fundamental assumption of a closed isochoric system. However, fluid inclusions in strongly recrystallized crystals may have lost most of their petrographic evidence for post-entrapment modification. Limited analytical data indicates that even those inclusions with modified total salinity and/or volume still contain basically unchanged cation ratios.

Acknowledgements We would like to thank Christoph Heinrich for his great support in this work, especially for the help in editing the manuscript and for the many fruitful discussions. Other useful suggestions have been given by Eiken Haussühl and Martin Kunz (both at the Institute of Crystallography, ETH Zürich), and from John Ridley (Macquarie University, Sydney). This research was supported by ETH research grant 0-20-041-95.

References

Audétat A, Günther D, Heinrich CA (1998) Formation of a Magmatic-hydrothermal Ore Deposit: insights with LA-ICP-MS analysis of fluid inclusions. Science 279: 2091–2094

Bakker RJ, Diamond LW (1998) Reequilibration of synthetic CO_2-H_2O fluid inclusions in quartz. In: Vanko DA, Cline JS (eds) Pacrofi VII Abstracts, Las Vegas, p10

Bakker RJ, Jansen JBH (1990) Preferential water leakage from fluid inclusions by means of mobile dislocations. Nature 345: 58–60

Bakker RJ, Jansen JBH (1991) Experimental post-entrapment water loss from synthetic CO_2-H_2O inclusions in natural quartz. Geochim Cosmochim Acta 55: 2215–2230

Bakker RJ, Jansen JBH (1994) A mechanism for preferential H_2O leakage from fluid inclusions in quartz, based on TEM observations. Contrib Mineral Petrol 116: 7–20

Blacic JD (1975) Plastic-deformation mechanisms in quartz: the effect of water. Tectonophysics 27: 271–294

Bodnar RJ, Vityk MO (1994) Interpretation of microthermometric data for H_2O-NaCl fluid inclusions. In: De Vivo B, Frezzotti ML (eds) Fluid inclusions in minerals: methods and applications. Virginia Tech, Blacksburg, Va., pp 117–130

Boullier AM, Michot G, Pêcher A, Barres O (1989) Diffusion and/or plastic deformation around fluid inclusions in synthetic quartz: new investigations. In: Bridgewater D (ed) Fluid movements – element transport and the composition of the deep crust. NATO ASI Series, Kluwer Academic Publishers, Dordrecht, pp 345–360

Boullier AM, France-Lanord C, Dubessy J, Adamy J, Champenois M (1991) Linked fluid and tectonic evolution in the High Himalayan Mountains (Nepal). Contrib Mineral Petrol 107: 358–372

Chou IM (1983) Migration of brine inclusions in single crystals of NaCl. U.S. Geological Survey Professional Paper, Report P1375

Cohen JA (1989) New data on the cause of smoky and amethystine color in quartz. Mineral Rec 20: 365–367

Cordier P, Doukhan JC, Ramboz C (1994) Influence of dislocations on water-loss from fluid inclusions in quartz: a quantitative reappraisal. Eur J Mineral 6: 745–752

Doukhan JC, Trépied L (1985) Plastic deformation of quartz single crystals. Bull Minéral 108: 97–123

FitzGerald JD (1991) Microstructures in water-weakened single crystals of quartz. J Geophys Res 96: 2139–2155

Gratier JP, Jenatton L (1984) Deformation by solution-deposition, and re-equilibration of fluid inclusions in crystals depending on temperature, internal pressure and stress. J Struct Geol 6: 189–200

Günther D, Audétat A, Frischknecht R, Heinrich CA (1998) Quantitative analysis of major, minor and trace elements in fluid inclusions using laser ablation inductively coupled-plasma mass spectrometry. J Anal At Spectrom 13: 263–270

Hall DL, Sterner SM (1993) Preferential water loss from synthetic fluid inclusions. Contrib Mineral Petrol 114: 489–500

Hartley NEW, Wilshaw TR (1973) Deformation and fracture of synthetic α-quartz. J Materials Science 8: 265–278

Hoekstra P, Osterkamp TE, Weeks WF (1965) The migration of liquid inclusions in single ice crystals. J Geophys Res 70: 5035–5041

Hollister LS (1990) Enrichment of CO_2 in fluid inclusions in quartz by removal of H_2O during crystal-plastic deformation. J Struct Geol 12: 895–901

Johnson EL, Hollister LS (1995) Syndeformational fluid trapping in quartz: determining the pressure-temperature conditions from fluid inclusions and the formation of pure CO_2 fluid inclusions during grain-boundary migration. J Metamorph Geol 13: 239–249

Martin JJ, Halliburton LE, Bossoli RB, Armington AF (1982) Influence of crystal growth rate and electrodiffusion (sweeping) on point defects in alpha-quartz. In: Proceedings of the Sym-

posium on Frequency Control (36th Annual), 2–4 June 1982, Philadelphia, Pa., pp 77–81
Mavrogenes JA, Bodnar RJ (1994) Hydrogen movement into and out of fluid inclusions in quartz: experimental evidence and geologic implications. Geochim Cosmochim Acta 58: 141–148
Morgan GB, Chou IM, Pasteris JD, Olsen SN (1993) Re-equilibration of CO_2 fluid inclusions at controlled hydrogen fugacities. J Metamorph Geol 11: 155–164
Pêcher A (1981) Experimental decrepitation and re-equilibration of fluid inclusions in synthetic quartz. Tectonophysics 78: 567–583
Qin Z, Lu F, Anderson AT (1992) Diffusive re-equilibration of melt and fluid inclusions. Am Mineral 77: 565–576
Ridley J, Hagemann SG (1998) Interpretation of post-entrapment fluid inclusion re-equilibration at the Three Mile Hill, Marvel Loch and Griffins Find high-temperature Lode-gold deposits, Yilgarn Craton, Western Australia. Chem Geol (in press)
Roedder E (1971) Metastability in fluid inclusions. Soc Mining Geol Jpn Spec Issue 3: 327–334
Roedder E (1984) Fluid inclusions. (Reviews in Mineralogy 12) Geol. Soc. Am., Washington DC
Roedder E, Belkin HE (1980) Thermal gradient migration of fluid inclusions in single crystals of salt from the waste isolation pilot plant site (WIPP). Sci Basis Nucl Waste Manage 2: 453–464
Rykart R (1989) Quarz-Monographie. Ott Verlag Thun, Switzerland
Sheftal NN, Gavrilova IV (1966) Equilibrium shape of a crystal in relation to the bulk free energy. In: Bradley JES (ed) Growth of crystals Vol. 4, Consultants Bureau Incorporation, New York, pp 24–26
Spencer WJ, Haruta WJ (1966) Defects in synthetic quartz. J Appl Physics 37: 549–553
Sterner SM, Bodnar RJ (1989) Synthetic fluid inclusions VII. Re-equilibration of fluid inclusions in quartz during laboratory-simulated metamorphic burial and uplift. J Metamorph Geol 7: 243–260
Sterner SM, Hall DL, Keppler H (1995) Compositional re-equilibration of fluid inclusions in quartz. Contrib Mineral Petrol 119: 1–15
Swanenberg HEC (1980) Fluid inclusions in high-grade metamorphic rocks from SW Norway. PhD. Thesis Geol. Ultraiectina Univ. Utrecht 25: 1–147
Twiss RJ (1976) Some planar deformation features, slip systems, and submicroscopic structures in synthetic quartz. J Geol 84: 701–724
Vityk MO (1998) Plastic flow associated with reequilibration of fluid inclusions in quartz. In: Vanko DA, Cline JS (eds) Pacrofi VII Abstracts, Las Vegas, p 69
Vityk MO, Bodnar RJ (1995) Textural evolution of synthetic fluid inclusions in quartz during reequilibration, with application to tectonic reconstruction. Contrib Mineral Petrol 121: 309–323
Wilke KT, Bohm J (1988) Kristallzüchtung. Harri Deutsch Verlag, Thun, Switzerland
Yoshimura J, Miyazaki T, Wada T, Kohra K, Hosaka M, Ogawa T, Taki S (1979) Measurement of local variations in spacing and orientations of lattice plane of synthetic quartz. J Crystal Growth 46: 691–700